Electronic Supplementary Information

Mechanism of water oxidation by [Ru(bda)(L)$_2$]: the return of the "blue dimer".

Javier J. Concepcion,*,† Diane K. Zhong,† David J. Szalda,¥ James T. Muckerman,† Etsuko Fujita†

† Department of Chemistry, Brookhaven National Laboratory. ¥ Department of Natural Sciences, Baruch College, CUNY, New York, New York 10010

Index

Experimental.

Materials. High-purity water was obtained by passing house-distilled water through a Millipore Milli-Q Synthesis A-10 system. Perchloric acid (70%, Aldrich, 99.999% trace metals grade) was used to prepare 0.1 M $HClO_4$. Di-μ-chlorobis-[(η^6-benzene)chlororuthenium(II)] ([(Ru(benzene)Cl)$_2$Cl$_2$])[1] and 2,2'-bipyridine-6,6'-dicarboxylic acid ($bdaH_2$)[2] were synthesized as reported in the literature.

Instrumentation.

NMR spectra were recorded at room temperature on a Bruker Avance spectrometer operating at 400 MHz. Chemical shifts are reported in parts per million (ppm) referenced to the residual solvent peak. Reported pH values were measured on a Fisher Scientific *accumet* Micro glass electrode after calibration with standard buffer solutions. Electronic absorption spectra were recorded with a UV-visible Agilent 8453 diode-array spectrophotometer and were corrected for the background spectrum of the solvent. Elemental analyses were performed by Robertson Microlit Laboratories. Electrochemical measurements were made with a CH Instruments CH-760E potentiostat at room temperature (22 ± 1 °C). Voltammetric studies were performed in a single compartment cell on glassy carbon disc (GC) or fluorine doped tin oxide (FTO) planar working electrodes with a Ag/AgCl (3 M NaCl) reference electrode and platinum wire counter electrode. An electrolyte filled bridge tube fitted with a Vycor tip (Bioanalytical Systems Inc., MF-2042) was employed when exclusion of chloride ion was desired. Electrochemical preparations of Ru(III) catalyst samples were performed in a bulk electrolysis cell (Bioanalytical Systems Inc., MF-1056) on a large surface area reticulated vitreous carbon (RVC) electrode. Rotating ring-disc electrode (RRDE) experiments were performed with a Pine Instruments bipotentiostat and rotator. The working electrode was the previously described *nano*-ITO or *nano*-ATO modified ring-disc electrode (*nano*-ITO-RRDE). The reference electrode was a standard Ag/AgCl electrode (PINE model RREF0021) mounted in a Vycor tipped glass tube with fresh electrolyte to avoid chloride contamination of the primary electrolyte. The counter electrode was a platinum wire coil in an isolated glass tube with fine glass frit separator (PINE model AFCTR5). All the experiments were performed with 0.1 M $HClO_4$ following literature procedures.[3]

Methods.

Synthesis and characterization.

[Ru(bda)(pic)$_2$]•H_2O. [(Ru(benzene)Cl)$_2$Cl$_2$], 307 mg (0.614 mmol), $bdaH_2$, 300 mg (1.23 mmol) and methanol (30 mL) were added to a three-neck round bottom flask. The mixture was degassed with argon and refluxed for 2 hours. 4-picoline (1.0 mL) was added followed by triethylamine (1.5 mL) and refluxed was continued overnight. The reaction mixture was allowed to cool to room temperature and filtered to separate an orange solid, presumably *trans*-[Ru(pic)$_4$Cl$_2$] based on ^{1}H NMR. The filtrate was taken to dryness by rotary evaporation and acetone was added. The solid was collected by filtration and washed with acetone until the washings were clear. The solid was dissolved in chloroform and washed with aqueous ascorbic acid (two times) and with water. The organic phase was dried with

magnesium sulfate, filtered and taken to dryness by rotary evaporation. The solid was collected to yield 521 mg, 80% of [Ru(bda)(pic)$_2$]. Elemental analysis calculated for [Ru(bda)(pic)$_2$]•H_2O, $C_{24}H_{22}N_4O_5Ru$ (MW 547.53): C 52.65; H 4.05; N 10.23; Found: C 52.10, H 3.81, N 10.21.

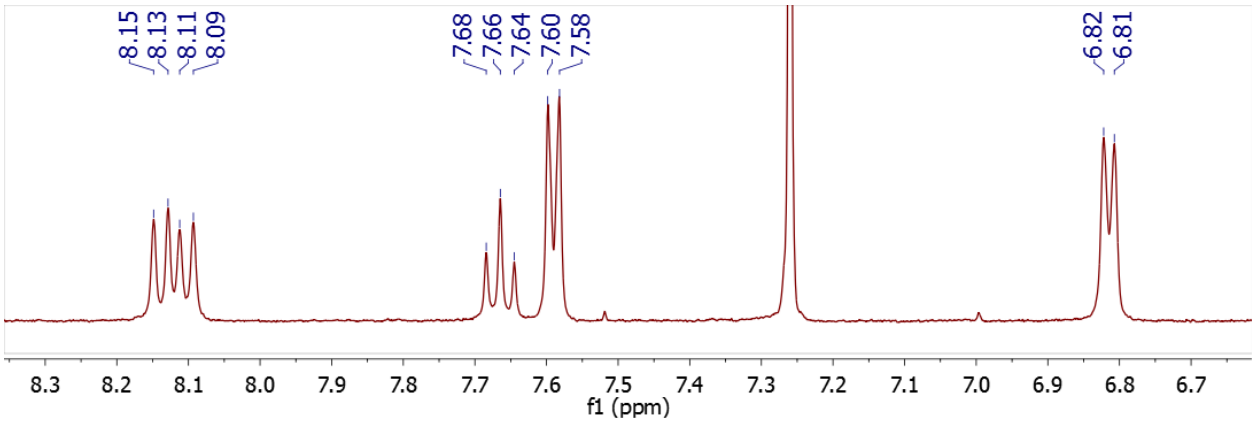

Figure S1. ^{1}H NMR for **[Ru(bda)(pic)$_2$]** in $CDCl_3$.

[Ru(bda)(isoq)$_2$]•0.5H_2O. [(Ru(benzene)Cl)$_2$Cl$_2$], 307 mg (0.614 mmol), bdaH_2, 300 mg (1.23 mmol) and methanol (30 mL) were added to a three-neck round bottom flask. The mixture was degassed with argon and refluxed for 3 hours. Isoquinoline (2.0 mL) was added followed by triethylamine (1.5 mL) and refluxed was continued overnight. The reaction mixture was allowed to cool to room temperature and filtered to separate an orange solid, presumably *trans*-[Ru(isq)$_4$Cl$_2$] based on ^{1}H NMR. The filtrate was taken to dryness by rotary evaporation and acetone was added. The solid was collected by filtration and washed with acetone until the washings were clear. The solid was dissolved in chloroform and washed with aqueous ascorbic acid (two times) and with water. The organic phase was dried with magnesium sulfate, filtered and taken to dryness by rotary evaporation. The solid was collected to yield 630 mg, 85% of [Ru(bda)(isq)$_2$]. Elemental analysis calculated for [Ru(bda)(isoq)$_2$]•0.5H_2O, $C_{30}H_{21}N_4O_{4.5}Ru$ (MW 610.59): C 59.01; H 3.47; N 9.18; Found: C 59.20, H 3.58, N 9.21.

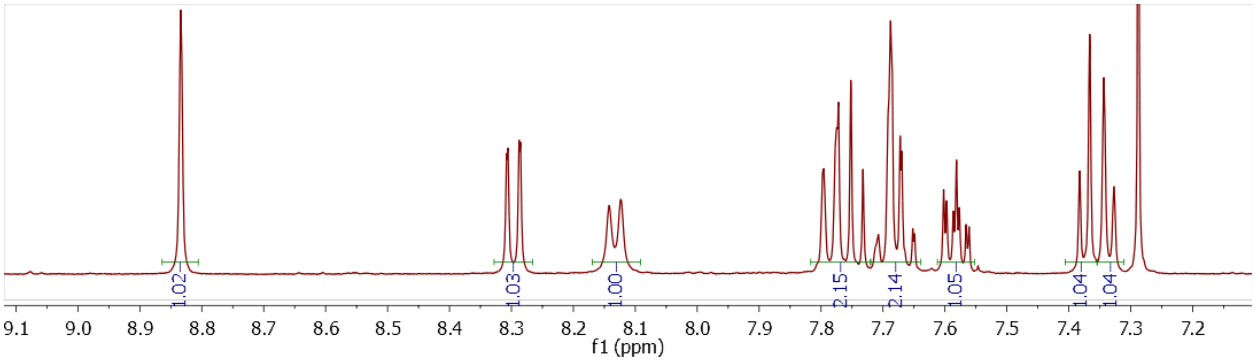

Figure S2. ^{1}H NMR for **[Ru(bda)(isq)$_2$]** in $CDCl_3$.

[Ru(bda)(pic)$_2$](ClO$_4$)•3H_2O. [Ru(bda)(pic)$_2$] (50 mg, 0.094 mmol) was dissolved in 0.1 M $HClO_4$ solution containing 20% CH_3CN. Controlled potential electrolysis past the Ru^{III}/Ru^{II} couple (0.75 V vs Ag/AgCl) was carried out until ~ 1 eq of charge was passed in a bulk electrolysis cell (Bioanalytical Systems Inc., **MF-1056**). Aqueous sodium perchlorate was

added and the CH_3CN was removed by rotary evaporation. After cooling the yellow precipitate was collected by filtration, washed with water and air dried. **Caution!** Perchlorate salts are potentially explosive! Do not rinse the solid with organic solvents! Yield: 52 mg, 76%. Elemental analysis calculated for $[Ru(bda)(pic)_2](PF_6)\bullet 3H_2O$, $C_{24}H_{26}F_6N_4O_7PRu$ (MW 728.53): C 39.57; H 3.60; N 7.69; Found: C 39.55, H 3.13, N 7.25. Single crystals for X-ray analysis were grown by slow diffusion of diethyl ether into a solution of the complex in CH_3CN.

$[Ru(bda)(isq)_2](ClO_4)\bullet 3H_2O$. $[Ru(bda)(pic)_2]$ (50 mg, 0.094 mmol) was dissolved in 0.1 M $HClO_4$ solution containing 20% CH_3CN. Controlled potential electrolysis past the Ru^{III}/Ru^{II} couple (0.8 V vs Ag/AgCl) was carried out until ~ 1 eq of charge was passed in a bulk electrolysis cell (Bioanalytical Systems Inc., **MF-1056**). Aqueous sodium perchlorate was added and the CH_3CN was removed by rotary evaporation. After cooling the yellow precipitate was collected by filtration, washed with water and air dried. **Caution!** Perchlorate salts are potentially explosive! Do not rinse the solid with organic solvents! Yield: 52 mg, 76%. Elemental analysis calculated for $[Ru(bda)(isq)_2](ClO_4)\bullet 3H_2O$, $C_{24}H_{26}F_6N_4O_7PRu$ (MW 728.53): C 39.57; H 3.60; N 7.69; Found: C 39.55, H 3.13, N 7.25. Single crystals for X-ray analysis were grown by slow diffusion of diethyl ether into a solution of the complex in CH_3CN.

(1-(pyridin-4-yl)ethane-1,2-diyl)bis(phosphonic acid), P_2-py. The synthesis of this ligand was carried out in three steps starting from 4-vinylpyridinium triflate, Figure S3.

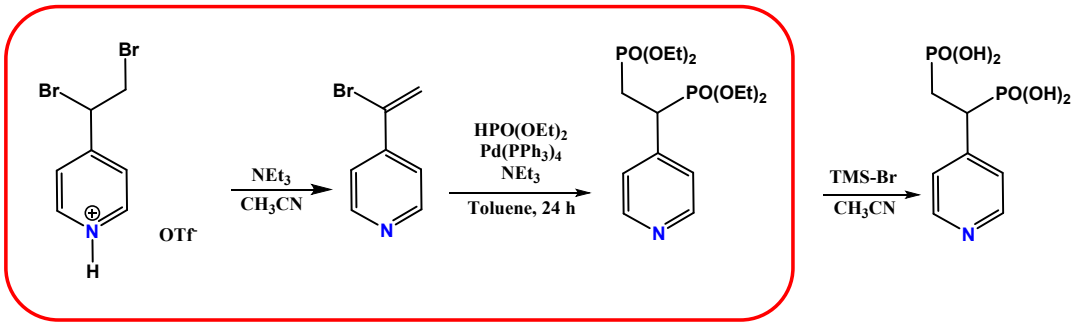

Figure S3. Synthetic scheme for the synthesis of **P_2-py**.

4-vinylpyridinium triflate. 4-vinylpyridine (5.0 g, 47.6 mmol) was dissolved in diethyl ether and cooled in an ice bath. Excess triflic acid was added drop wise under magnetic stirring and the resulting white precipitate was filtered, rinsed with diethyl ether and air dried. Yield: 11.2 g, 92%.

4-(1',2'-dibromoethyl)pyridinium triflate. This compound was prepared by a modification of a reported procedure.[4] 4-vinylpyridinium triflate (8.0 g, 31.3 mmol) in chloroform (30 mL) was cooled in an ice bath and bromine (10.0 g, 62.6 mmol) was added drop wise with under magnetic stirring. After the addition was finished, the reaction mixture was stirred at ice bath temperature for an hour followed by another hour at room temperature. Excess diethyl ether

was added and the orange precipitate was filtered and rinsed with diethyl ether. Yield: 10.6 g, 82%.

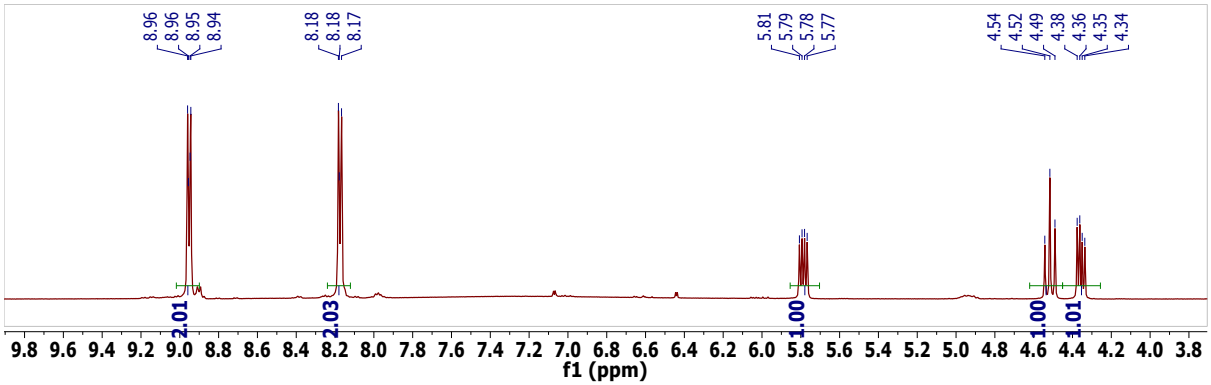

Figure S4. ^{1}H NMR for 4-(1′,2′-dibromoethyl)pyridinium triflate in DMSO-d_6.

4-(1'-bromoethenyl)pyridine. 4-(1′,2′-dibromoethyl)pyridinium triflate (8.0 g, 19.3 mmol) was dissolved in anhydrous acetonitrile and cooled in an ice bath. Triethylamine (9.8 g, 96.5 mmol) was added slowly via syringe. The reaction mixture was stirred at ice bath temperature for an hour and at room temperature for 2 hours. All volatiles were removed by rotary evaporation and water was added to the residue. The aqueous solution was extracted with diethyl ether (5x30 mL), dried over magnesium sulfate and filtered. The diethyl ether was removed by rotary evaporation to yield light yellow oil. This compound was used in the next step without additional purification. Yield: 3.0 g, 85%.

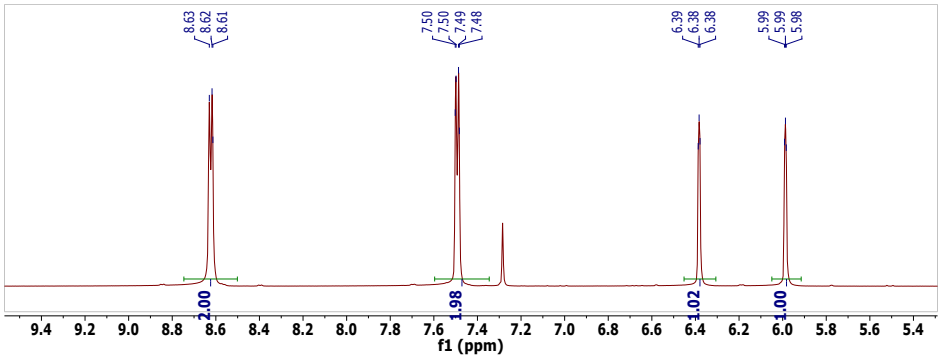

Figure S5. ^{1}H NMR for 4-(1′-bromoethenyl)pyridine in $CDCl_3$.

Tetraethyl (1-(pyridin-4-yl)ethane-1,2-diyl)bis(phosphonate). 4-(1′-bromoethenyl)pyridine (2.5 g, 13.6 mmol) and $Pd(PPh_3)_4$ (1.62 g, 1.4 mmol) were dissolved in anhydrous toluene (30 mL) using Schlenk techniques. Previously degassed diethylphosphite (40.8 mmol) and triethylamine (54.4 mmol) were added via syringe and the mixture was degassed by bubbling argon. The mixture was heated at 100 °C for 24 hours, cooled and filtered. All volatiles in the filtrate were removed by rotary evaporation and the oily residue was loaded on a silica gel column and eluted with CH_2Cl_2:NEt_3:MeOH (90:7:3). The desired product was obtained as a clear oil. Yield: 3.35 g, 65%.

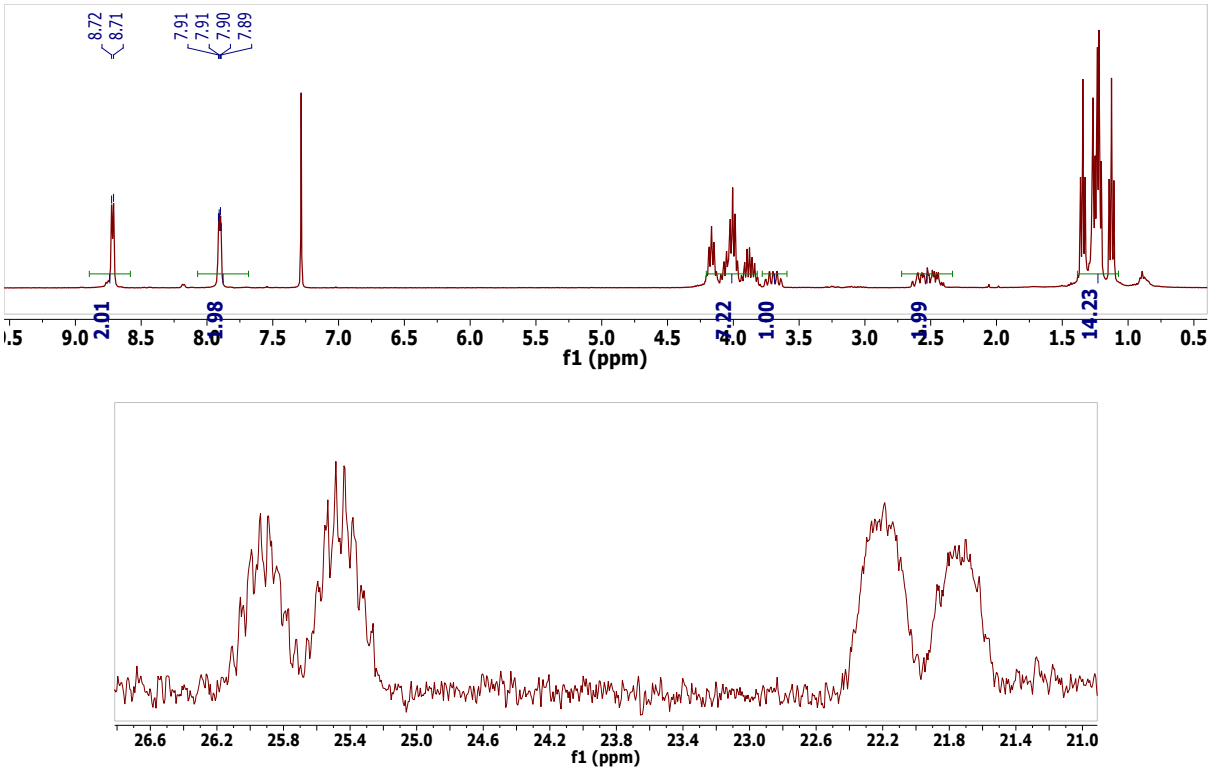

Figure S6. ^{1}H NMR and ^{31}P NMR for tetraethyl(1-(pyridin-4-yl)ethane-1′,2′-diyl)bis(phosphonate) in $CDCl_3$.

(1-(pyridin-4-yl)ethane-1,2-diyl)bis(phosphonic acid), ***P_2-py***. Tetraethyl(1-(pyridin-4-yl)ethane-1′,2′-diyl)bis(phosphonate) (3.0 g, 7.9 mmol) was dissolved in anhydrous acetonitrile (30 mL) using Schlenk techniques. Bromotrimethylsilane (5.44 g, 35.6 mmol) was added with a syringe and the mixture heated at 70 °C for 48 h. Anhydrous methanol (3.0 mL) was added and the mixture was allowed to cool to room temperature under magnetic stirring. The white solid was filtered and rinsed with acetonitrile. Yield: 1.96 g, 93%. ^{1}H NMR (400 MHz, D_2O-NaOD): δ 8.31 (d, 2H), 7.42 (d, 2H), 3.34-3.03 (m, 1H), 2.18-1.99 (m, 2H).

[Ru(bda)(P_2-py)$_2$]. [(Ru(benzene)Cl)$_2$Cl$_2$], 307 mg (0.614 mmol), bdaH_2, 300 mg (1.23 mmol) and methanol (30 mL) were added to a three-neck round bottom flask. The mixture was degassed with argon and refluxed for 2 hours. P_2-py (1.31 g, 4.92 mmol) was added followed by triethylamine (1.5 mL) and refluxed was continued for 48 h. The reaction mixture was allowed to cool to room temperature and filtered to separate an orange solid, presumably *trans*-[Ru(pic)$_4$Cl$_2$] based on ^{1}H NMR. The filtrate was taken to dryness by rotary evaporation and acetone was added. The solid was collected by filtration and washed with acetone until the washings were clear. The solid was suspended in degassed acetone and refluxed under argon for an hour. The mixture was filtered hot and the solid washed with acetone and diethyl ether. Yield 733 mg, 68%. ^{1}H NMR (400 MHz, D_2O-NaOD): δ 8.50 (d, 2H), 7.96-7.89 (m, 4H), 7.70 (d, 4H), 7.13 (d, 4H), 3.15-3.11 (m, 2H), 2.38-2.06 (m, 4H).

Theoretical calculations. Theoretical calculations were carried out using Density Functional Theory (DFT) as implemented in Gaussian09, revision D.01.[5] Becke's three-parameter

hybrid functional[6-9] with the LYP correlation functional[10] (B3LYP) was used. The LANL2 relativistic effective core potential[11] and associated uncontracted basis set was used for Ru and the 6-311G(5d,p) basis set for C, N, O, and H. The solvent (water) was modeled by means of the Integral Equation Formalism Polarizable Continuum Model (IEF-PCM)[12-15], as implemented in Gaussian09. Universal Force Field radii (UFF) were used in all cases. Frequency calculations were performed to ensure that each optimized structure is a local minimum on the potential energy surface and to extract Gibbs free energies. For non-gases, the latter were corrected by adding $\Delta G^{o\rightarrow *} = RT \ln(24.46) = 1.894$ kcal/mol to convert from the quantum chemical standard state of 1.0 atm of pressure in the gas phase to 1.0 M in solution.[16,17] For added water molecules, $\Delta G^{*}_{self} = -3.947$ kcal/mol and $\Delta G^{o\rightarrow *} = +1.894$ kcal/mol were added to the gas phase Gibbs free energy to convert from the quantum chemical standard state of 1.0 atm of pressure in the gas phase to the vapor pressure of the pure liquid solvent.[16,17] Franck-Condon vertical excitation energies and oscillator strengths were obtained with non-equilibrium Time-Dependent Density Functional Theory (TD-DFT)[18-20] as implemented in Gaussian09.

Table S1. Selected bond distances (Å) for $[Ru^{II}(bda)(pic)_2]$ and $[Ru^{III}(bda)(pic)_2]^+$.

Complex	$[Ru^{II}(bda)(pic)_2]$	$[Ru^{III}(bda)(pic)_2]^+$
Ru–O1	2.216(7)	2.050(2)
Ru–O2	2.172(7)	2.063(2)
$Ru–N1_{bpy}$	1.950(8)	1.994(2)
$Ru–N2_{bpy}$	1.914(7)	1.995(2)
$Ru–N1_{pic}$	2.070(6)	2.081(2)
$Ru–N2_{pic}$	2.084(6)	2.072(2)

$[Ru^{III}(\kappa^4\text{-bda})(pic)_2]^+$ $[Ru^{III}(\kappa^3\text{-bda})(pic)_2(OH_2)]^+$

Figure S7. Optimized structures of $[Ru^{III}(\kappa^4\text{-bda})(pic)_2]^+$ and $[Ru^{III}(\kappa^3\text{-bda})(pic)_2(OH_2)]^+$.

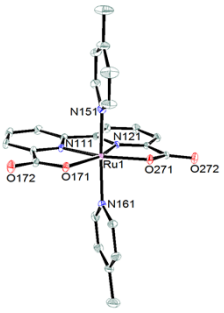

Figure S8. X-ray structure of $[Ru^{III}(bda)(pic)_2]^+$ in the salt $[Ru(bda)(pic)_2](ClO_4)$. Oxidation from Ru^{II} to Ru^{III} results in significant shortening of the Ru-O distances ($\Delta d = -0.14$ Å) and elongation of the Ru–N(bpy) distances ($\Delta d = +0.06$ Å). But the Ru-N(pic) distances remain unaffected; most of the geometrical changes take place in the equatorial plane. The O–Ru–O bite angle increases from 123.0 to 126.4°.

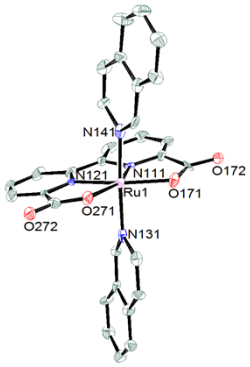

Figure S9. X-ray structure of $[Ru^{III}(bda)(isq)_2]^+$ in the salt $[Ru(bda)(isq)_2](ClO_4)$.

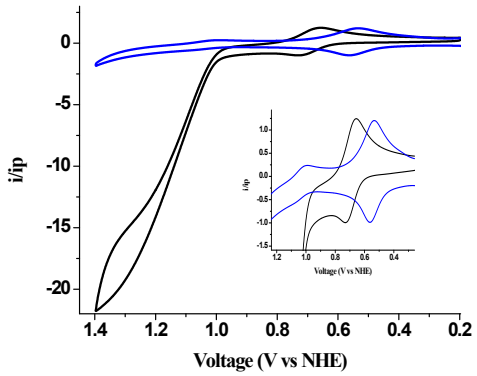

Figure S10. Cyclic voltammograms for 1.0 mM **[Ru(bda)(pic)$_2$]** (black trace) in solution with a glassy carbon electrode and **[Ru(bda)(P$_2$-py)$_2$]** (blue trace) on an FTO electrode in 0.1 M pH 8.0 phosphate buffer. The currents have been normalized for $\nu^{1/2}$ and ν, respectively, and then for the $Ru^{IV/II}$ peak current. The inset is an expansion of the $Ru^{IV/II}$ couple.

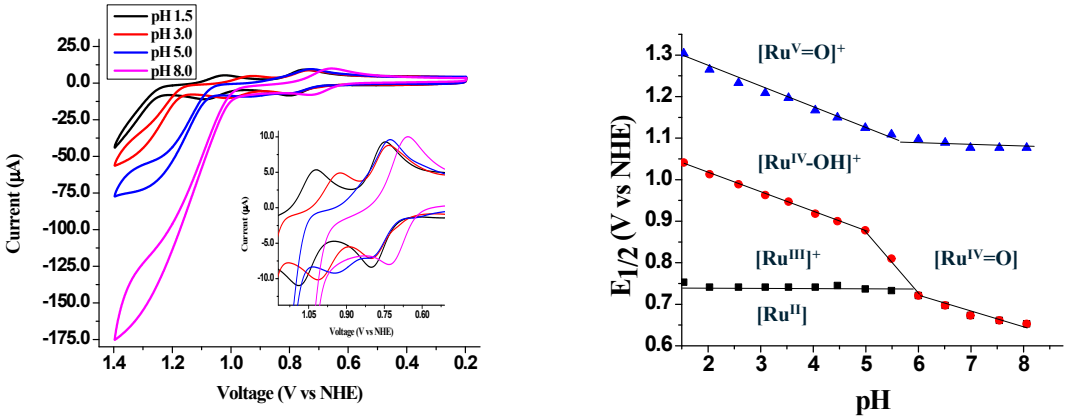

Figure S11. Representatives CVs at various pHs and $E_{1/2}$ *vs* pH plot for **[Ru(bda)(pic)$_2$]**.

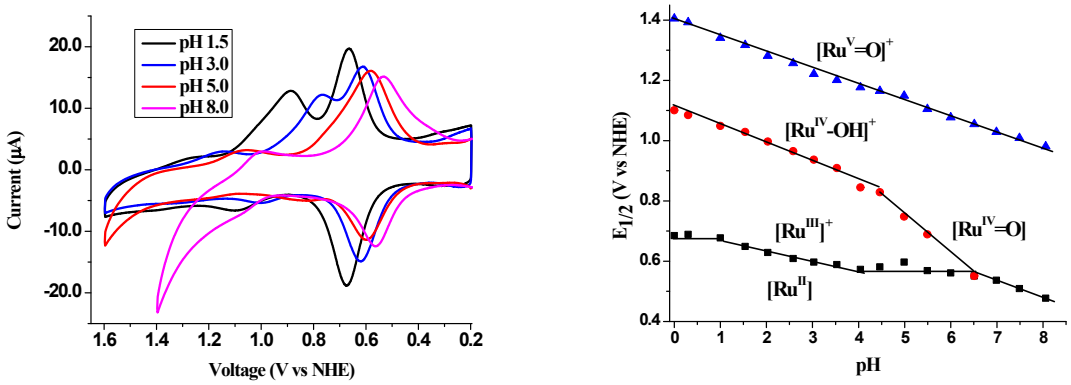

Figure S12. Representatives CVs at various pHs and $E_{1/2}$ vs pH plot for **[Ru(bda)(P$_2$-py)$_2$]**.

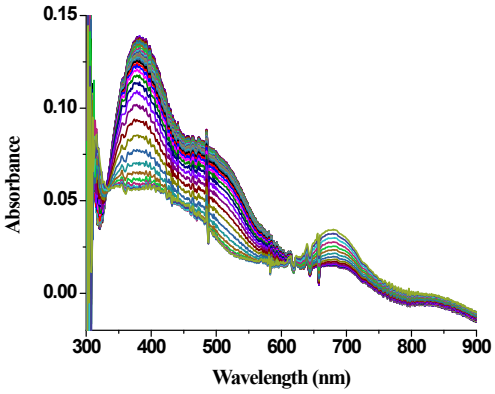

Figure S13. Spectral changes associated with oxidation of Ru^{II} to Ru^{III} in Figure 3.

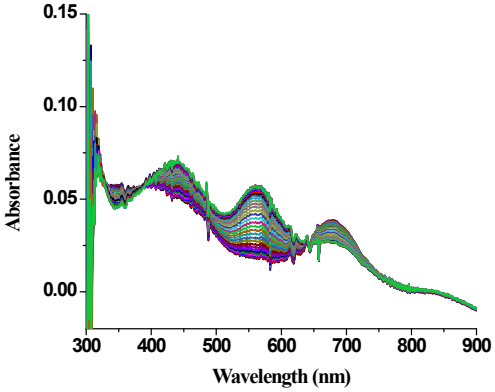

Figure S14. Spectral changes associated with oxidation of Ru^{III} to "Ru^{IV}" in Figure 3.

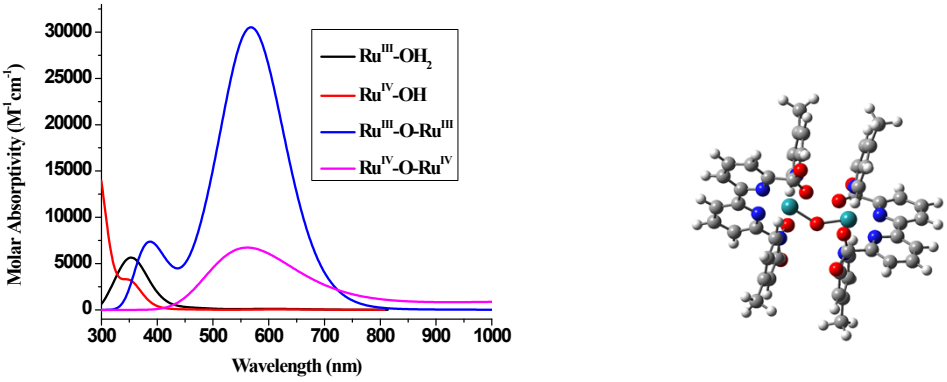

(A) **(B)**

Figure S15. (A) Predicted absorption spectra using TD-DFT for $[Ru^{III}(\kappa^3\text{-bda})(pic)_2(OH_2)]^+$ (Ru^{III}–OH_2), $[Ru^{IV}(bda)(pic)_2(OH)]^+$ (Ru^{IV}–OH), $[(\kappa^3\text{-bda})(pic)_2Ru^{III}ORu^{III}(\kappa^3\text{-bda})(pic)_2]$ (Ru^{III}–O–Ru^{III}) and $[(\kappa^3\text{-bda})(pic)_2Ru^{IV}ORu^{IV}(\kappa^3\text{-bda})(pic)_2]$ (Ru^{IV}–O–Ru^{IV}). (B) Optimized structure of $[(\kappa^3\text{-bda})(pic)_2Ru^{III}ORu^{III}(\kappa^3\text{-bda})(pic)_2]$ (Ru^{III}–O–Ru^{III}).

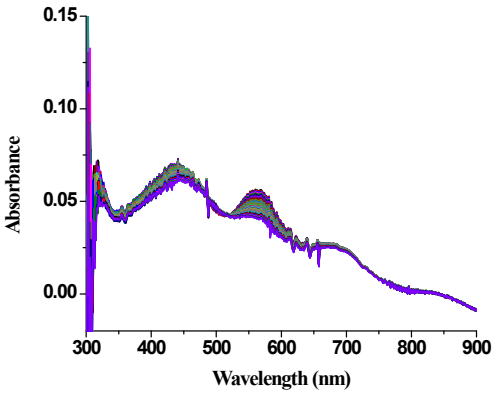

Figure S16. Spectral changes associated with the last oxidation process in Figure 3.

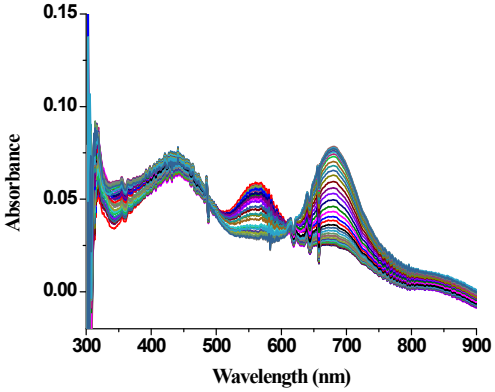

Figure S17. Spectral changes associated with the reduction process from 172 to 216 s in Figure 3.

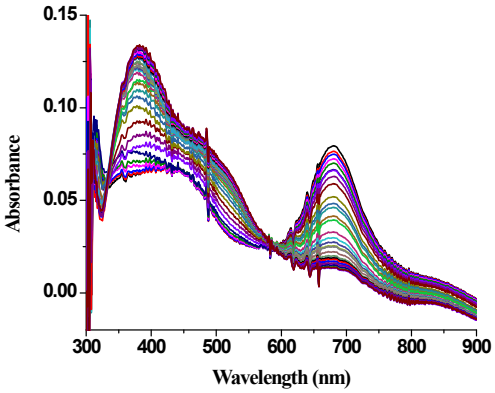

Figure S18. Spectral changes associated with the reduction process from 217 to 280 s in Figure 3.

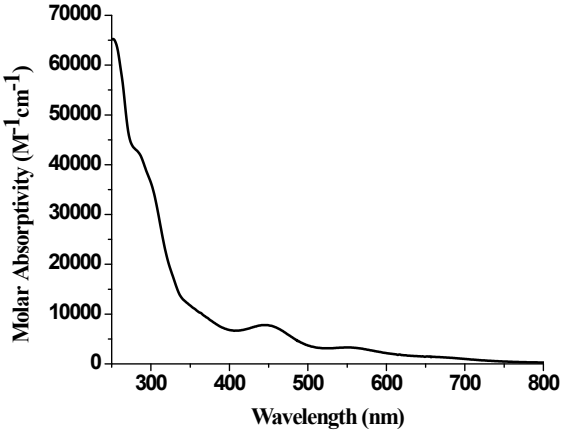

Figure S19. Absorption spectra for "$Ru^{IV}ORu^{IV}$" at pH 1.0. It was generated electrochemically from **[Ru(bda)(pic)$_2$]** by controlled-potential electrolysis at 1.2 V.

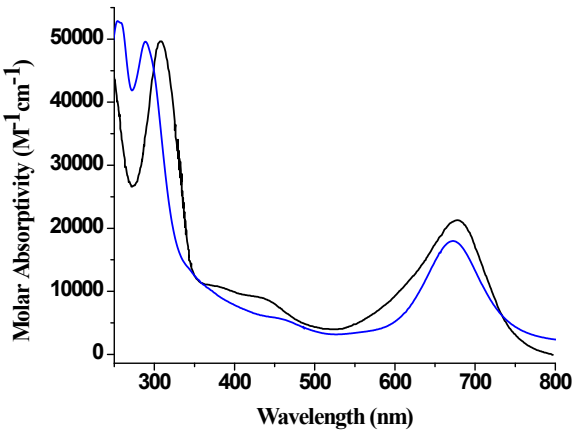

Figure S20. Absorption spectra for "$Ru^{III}ORu^{III}$" at pH 1.0. Blue: electrochemically generated "$Ru^{III}ORu^{III}$" from **[Ru(bda)(pic)$_2$]** by controlled-potential electrolysis at 1.2 V followed by reduction of the generated intermediate at 0.97 V. Black: $[(L)_2(H_2O)Ru^{III}ORu^{III}(OH_2)(L)_2]^{4+}$ (L is 2,2′-bipyridine-4,4′-dicarboxylic acid) according to Graetzel *et al.*, *J. Mol. Catal.* **1989**, *52*, 63.

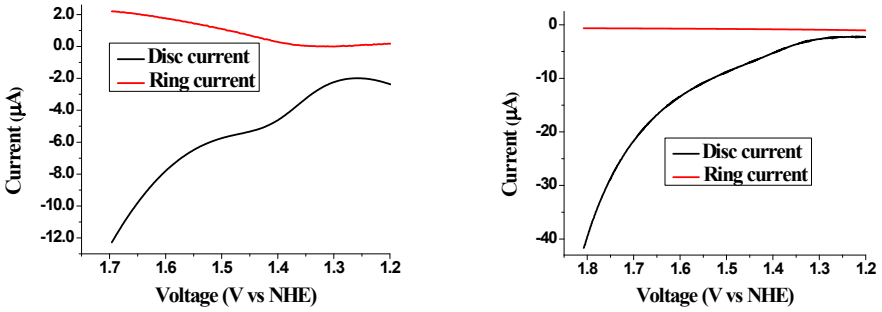

Figure S21. (A) Rotating ring disc voltammogram in 0.1 M $HClO_4$. The potential at the disc was scanned from 1.2 V to 1.7 V at 10 mV/s. The rotation rate was 500 rpm. The potential of the ring (platinum) was held constant at -0.017 V. Black: current with [Ru(bda)(P_2-py)$_2$] attached to *nano*-ITO-modified glassy carbon disc. Red: corresponding ring current with [Ru(bda)(P_2-py)$_2$] present on the modified disc electrode. The increase in cathodic current at the ring past 1.33 V indicates oxygen generation at the disc. The collection efficiency at the ring for this experiment is 12.5%.[4] This number accounts for the overall ring collection efficiency of 25% and the factor of 2 ratio between water oxidation to O_2 at the disc ($4e^-$) and O_2 reduction to H_2O_2 ($2e^-$) at the ring. **(B)** Rotating ring disc voltammogram in 0.1 M $HClO_4$. The potential at the disc was scanned from 1.2 V to 1.8 V at 10 mV/s. The rotation rate was 500 rpm. The potential of the ring (platinum) was held constant at +1.13 V where oxidation of H_2O_2 to O_2 at platinum is diffusion-limited. Black: current with [Ru(bda)(P_2-py)$_2$] attached to *nano*-ITO-modified glassy carbon disc. Red: corresponding ring current with [Ru(bda)(P_2-py)$_2$] present on the modified disc electrode. The absence of anodic current at the ring indicates that no H_2O_2 is generated at the disc. The collection efficiency at the ring for this experiment is 25 %.[4] This number accounts for the overall ring collection efficiency of 25% and the factor of 1 ratio between water oxidation to H_2O_2 at the disc ($2e^-$) and H_2O_2 oxidation to O_2 ($2e^-$) at the ring.

Collection and Reduction of X-Ray Data. Crystals of $[Ru(bda)(pic)_2](ClO_4)$ and $[Ru(bda)(isq)_2](ClO_4)$, were mounted on the end of a glass fibers. Data was collected with a Bruker Kappa Apex II diffactometer. Data collected at 173K indicated monoclinic symmetry and space group $P2_1$ for $[Ru(bda)(pic)_2](ClO_4)$ and orthorhombic symmetry and space group $P2_12_12_1$ for $[Ru(bda)(isq)_2](ClO_4)$. Crystal data and information about the data collection are provided in Table S2 and below.

Determination and Refinement of the Structure. The structure was solved[22] by Patterson heavy atom methods. In the least-squares refinement,[22] anisotropic temperature parameters were used for all the non-hydrogen atoms. Hydrogen atoms were placed at calculated positions and allowed to "ride" on the atom to which they were attached. The isotropic thermal parameters for the hydrogen atoms were determined from the atom to which they are attached. The data were corrected for absorption using the multi-scan method (SADABS).[23] Table 1 contains details of the data collection and refinement.

Structures. An ORTEP drawing of $[Ru(bda)(pic)_2](ClO_4)$ showing the number scheme used is presented in Figure S19. In $[Ru(bda)(pic)_2](ClO_4)$ there are two close contacts between H(162) and H(156) of the two picoline ligands to O172 (1–x, ½+y, 2–z) of a symmetry related complex. The dihedral angle between the two picoline ligands is 5.5°. There are also two C-H···O hydrogen bonds between H162 and 156 of the two picoline lingands and O172 (1–x, ½ + y, 2–z) of a symmetry related complex with H···O172 (1–x, ½ + y, 2–z) distances of 2.57 and 2.56 Å respectively. The Ru(1)···O172 (1–x, ½ + y, 2–z) distance is 3.794(2) Å. In the seven coordinate Ru(IV) complex previously reported the picoline distances in the hydrogen bonds to the coordinated water are H···O(3) 2.63 and 2.71 Å while the angle between picolines ligands is 80.4 degrees. In $[Ru^{II}(bda)(pic)_2]$ the H···O(2) distances between the picoline and a coordinated oxygen atom are 2.38 and 2.64 Å and the picoline twist angle 22.4 degrees.

An ORTEP drawing of $[Ru(bda)(isq)_2](ClO_4)$ showing the number scheme used is presented in Figure S20. The dihedral angle between the two isoquinoline ligands is 10.0°. In this complex the distance between the hydrogen of the isoquinoline and the coordinated oxygen atoms are 3.15 and 2.84 and 2.75 and 3.083 Å to O(171) and O(172), respectively.

Table S2. Crystallographic Collection and Refinement Data for $[Ru(bda)(pic)_2](ClO_4)$ and $[Ru(bda)(isq)_2](ClO_4)$.

	$[Ru(bda)(pic)_2](ClO_4)$	$[Ru(bda)(isq)_2](ClO_4)$
Formula	$C_{24}H_{20}O_8N_4ClRu$	$C_{30}H_{20}O_8N_4ClRu$
fw	628.96	701.02
temp	173(2) K	173(2) K
cryst. syst	Monoclinic	Orthorhombic
space group	$P2_1$	$P2_12_12_1$
a (Å)	10.0833(2)	7.6696(18)
b (Å)	9.8576(2)	11.321(2)
c (Å)	12.7262(3)	32.206(7)
α(deg)	90	90
β(deg)	95.3270(10)	90

γ(deg)	90	90
V (Å^3)	1259.48(5)	2796.3(11)
Z	2	4
μ	0.785 mm^{-1}	0.717 mm^{-1}
λ (Å)	0.71073	0.71073
ρ calc (g cm^{-3})	1.658	1.665
cryst. size (mm)	0.43 × 0.20 × 0.04	0.40 × 0.07 × 0.07
θ range (deg)	2.47 to 30.18	2.20 to 25.00
total no. of reflns	20199	32740
no. of independent reflns,	7318 [R(int) = 0.0337]	4903 [R(int) = 0.2023]
I≥3.0σ(I)	6424	3181
no. of parameters	343	415
Final R indices [I>3σ (I)]	R1 = 0.0310, wR2 = 0.0614	R1 = 0.0745, wR2 = 0.1497
R indices (all data)	R1 = 0.0419, wR2 = 0.0649	R1 = 0.1378, wR2 = 0.1693
Goodness-of-fit on F2	0.993	0.974
Absorption correction	Semi-empirical from equivalents	Semi-empirical from equivalents

$R1 = \Sigma||F_O|- |F_C||/ \Sigma|F_O|$; $wR2 = \{\Sigma[w(|F_O^2|- |F_C^2|)^2]/ \Sigma[w|F_O^2|^2]\}^{1/2}$

Table S3. Comparison of bond lengths [Å] and angles [deg] between $[Ru(bda)(pic)_2](ClO_4)$ and $[Ru(bda)(isq)_2](ClO_4)$.

	$[Ru(bda)(pic)_2](ClO_4)$	$[Ru(bda)(isq)_2](ClO_4)$
Ru(1)–N(111)	1.9945(19)	1.974(7)
Ru(1)–N(121)	1.995(2)	1.964(8)
Ru(1)–O(171)	2.0496(17)	2.046(7)
Ru(1)–O(271)	2.0626(18)	2.047(7)
Ru(1)–N(131)	2.072(3)	2.062(8)
Ru(1)–N(141)	2.0807(19)	2.093(9)
N(111)–Ru(1)–N(121)	77.59(8)	79.0(4)
N(111)–Ru(1)–O(171)	78.08(7)	78.0(3)
N(121)–Ru(1)–O(171)	155.59(7)	156.6(3)
N(111)–Ru(1)–O(271)	155.52(9)	155.8(3)
N(121)–Ru(1)–O(271)	77.96(7)	77.2(3)
O(171)–Ru(1)–O(271)	126.39(7)	126.0(3)
N(111)–Ru(1)–N(141)	90.78(12)	89.2(3)

N(121)–Ru(1)–N(141)	93.87(8)	96.2(3)
O(171)–Ru(1)–N(141)	88.45(8)	87.7(3)
O(271)–Ru(1)–N(141)	89.86(11)	89.3(3)
N(111)–Ru(1)–N(131)	95.66(8)	97.3(3)
N(121)–Ru(1)–N(131)	92.85(8)	97.4(3)
O(171)–Ru(1)–N(131)	87.54(8)	90.0(3)
O(271)–Ru(1)–N(131)	86.54(8)	86.3(3)
N(141)–Ru(1)–N(131)	171.56(10)	172.4(3)

For this table $[Ru(bda)(pic)_2](ClO_4)$ has been renumbered so N151 is N141 and N161 is N131.

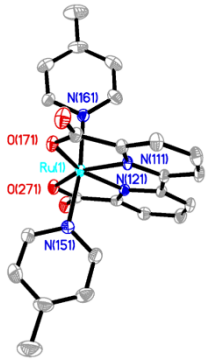

Figure S22. A view of $[Ru(bda)(pic)_2](ClO_4)$.

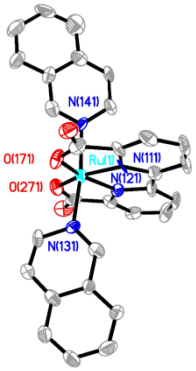

Figure S23. A view of $[Ru(bda)(isq)_2](ClO_4)$.

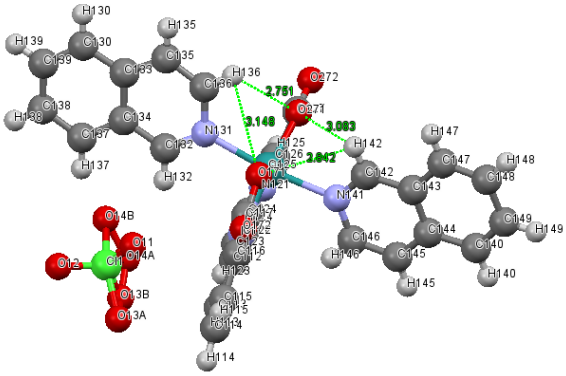

Figure S24. Close contacts for $[Ru(bda)(isq)_2](ClO_4)$.

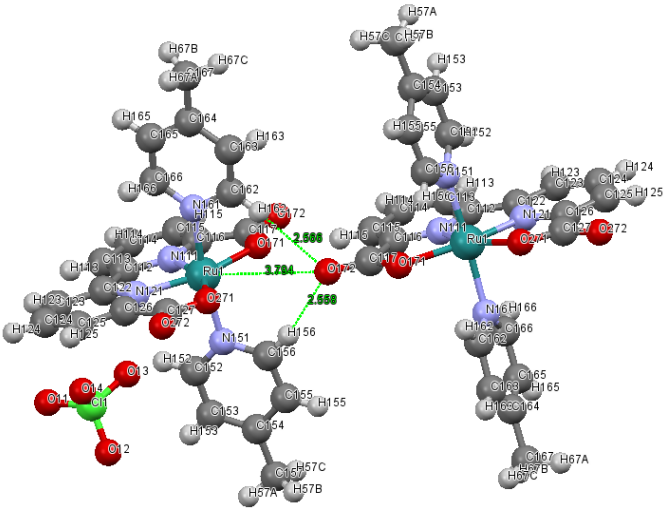

Figure S25. Close contacts for $[Ru(bda)(pic)_2](ClO_4)$.

Table S4. Cartesian coordinates for $[(\kappa^3\text{-bda})(pic)_2Ru^{III}ORu^{III}(\kappa^3\text{-bda})(pic)_2]$ (Ru^{III}–O–Ru^{III}).

Center Number	Atomic Number	Coordinates (Å) x	y	z
1	44	–1.816693	–0.062663	–0.139402
2	7	–3.730731	–0.701964	–0.600783

3	6	–6.208939	–1.701128	–1.252002
4	6	–4.759913	–0.470526	0.23502
5	6	–3.889879	–1.396311	–1.742791
6	6	–5.125549	–1.913074	–2.108516
7	6	–6.029414	–0.978735	–0.07375
8	1	–5.216973	–2.465368	–3.036336
9	1	–6.868263	–0.81795	0.591819
10	1	–7.189339	–2.09522	–1.498254
11	7	–3.078935	0.652604	1.57945
12	6	–5.033816	1.582072	3.380448
13	6	–2.738372	1.421055	2.637052
14	6	–4.409941	0.337396	1.416317
15	6	–5.391069	0.777441	2.299236
16	6	–3.700013	1.909838	3.539076
17	1	–6.427911	0.511517	2.138135
18	1	–3.368405	2.536235	4.360133
19	1	–5.788146	1.942013	4.072716
20	6	–2.618686	–1.55179	–2.544476
21	6	–1.286862	1.777837	2.956065
22	8	–0.666221	0.897096	3.598024
23	8	–0.928049	2.931524	2.621258
24	8	–1.566082	–1.026397	–1.980626
25	8	–2.6239	–2.140402	–3.625095
26	7	–2.282906	1.827989	–1.07711
27	6	–3.008508	4.328373	–2.172376
28	6	–2.883363	1.918377	–2.281161
29	6	–2.027046	2.977427	–0.417449
30	6	–2.378133	4.222372	–0.927388
31	6	–3.256653	3.128198	–2.850187
32	1	–3.066541	0.991034	–2.806758
33	1	–2.154626	5.109197	–0.341862
34	1	–3.739784	3.126486	–3.82239
35	7	–1.510926	–1.936446	0.898869
36	6	–1.47011	–4.360195	2.354359
37	6	–1.335247	–1.942992	2.238358
38	6	–1.634485	–3.130648	0.281105
39	6	–1.623161	–4.339666	0.961489
40	6	–1.311212	–3.119621	2.980181
41	1	–1.193355	–0.981258	2.721176
42	1	–1.725693	–3.109358	–0.795474
43	1	–1.728402	–5.261606	0.397938
44	1	–1.165132	–3.056361	4.054257
45	8	0.000049	0.560175	–0.00001
46	1	–1.539595	2.893349	0.548728
47	44	1.816772	–0.062656	0.139296
48	7	3.730821	–0.702042	0.600614
49	6	6.209035	–1.701301	1.2517
50	6	4.760013	–0.470486	–0.235143
51	6	3.889976	–1.396525	1.742537
52	6	5.125641	–1.913357	2.108183

53	6	6.029516	–0.97873	0.073558
54	1	5.217062	–2.465772	3.035932
55	1	6.868369	–0.817813	–0.591975
56	1	7.189433	–2.095428	1.497902
57	7	3.079027	0.652816	–1.579378
58	6	5.033909	1.582973	–3.380014
59	6	2.738441	1.42154	–2.636772
60	6	4.41005	0.337658	–1.416286
61	6	5.391171	0.777994	–2.299061
62	6	3.700096	1.910729	–3.538568
63	1	6.428016	0.512035	–2.138035
64	1	3.368475	2.53739	–4.359418
65	1	5.788243	1.943176	–4.072142
66	6	2.618818	–1.551981	2.544259
67	6	1.28689	1.778035	–2.955945
68	8	0.92779	2.931661	–2.621265
69	8	0.666544	0.897097	–3.597922
70	8	1.566233	–1.026419	1.980512
71	8	2.624019	–2.140669	3.624833
72	7	2.28292	1.827932	1.07713
73	6	3.008083	4.328307	2.172691
74	6	2.883415	1.918273	2.281166
75	6	2.02685	2.977401	0.417607
76	6	2.377729	4.222347	0.927691
77	6	3.256476	3.128091	2.850345
78	1	3.066814	0.990887	2.806615
79	1	2.154065	5.109205	0.342275
80	1	3.739626	3.126348	3.822538
81	7	1.510905	–1.936393	–0.89901
82	6	1.470114	–4.360185	–2.354435
83	6	1.633823	–3.130605	–0.281137
84	6	1.335796	–1.942953	–2.238575
85	6	1.311798	–3.119594	–2.980372
86	6	1.622495	–4.339642	–0.961492
87	1	1.724471	–3.109281	0.795487
88	1	1.16621	–3.056333	–4.054515
89	1	1.727199	–5.261591	–0.397855
90	1	1.539398	2.893355	–0.54857
91	6	–3.376647	5.662704	–2.765279
92	1	–4.23831	5.578286	–3.434229
93	1	–2.540413	6.060944	–3.354451
94	1	–3.606176	6.395566	–1.9859
95	6	–1.486568	–5.650336	3.130825
96	1	–0.937218	–6.43719	2.60356
97	1	–2.516888	–6.0056	3.260477
98	1	–1.049966	–5.524026	4.125576
99	6	3.375964	5.662625	2.765785
100	1	2.539819	6.060392	3.355403
101	1	3.604914	6.395775	1.986509
102	1	4.237922	5.578351	3.434375

103	6	1.486624	–5.650356	–3.130848
104	1	2.516907	–6.005963	–3.259857
105	1	1.050664	–5.523941	–4.125867
106	1	0.936697	–6.437013	–2.603889
107	1	1.19424	–0.981203	–2.721458

Table S5. Cartesian coordinates for $[Ru^{III}(\kappa^3\text{-bda})(pic)_2(OH_2)]^+$ (Ru^{III}–OH_2).

Center Number	Atomic Number	Coordinates (Å) x	y	z
1	1	–0.389348	–0.158951	4.536759
2	6	–0.366807	–0.778495	3.651874
3	6	–0.29371	–2.344326	1.394158
4	6	–0.201071	–0.207991	2.386756
5	6	–0.500554	–2.157982	3.76227
6	6	–0.461855	–2.960656	2.621211
7	7	–0.176953	–1.009896	1.308664
8	1	–0.629215	–2.607254	4.738429
9	1	–0.552565	–4.037227	2.667473
10	7	0.130704	1.531268	0.745578
11	6	0.108841	3.533681	2.689396
12	6	–0.035248	1.221517	2.074143
13	6	0.270054	2.826315	0.387385
14	6	0.23945	3.842273	1.347625
15	6	–0.033228	2.20088	3.057231
16	1	0.3209	4.862616	1.002246
17	1	–0.14672	1.927995	4.096354
18	1	0.107486	4.312352	3.441384
19	6	0.458982	3.270218	–1.079068
20	8	–0.075863	4.338126	–1.374479
21	6	–0.20393	–3.050508	0.059488
22	8	–0.317279	–4.253437	–0.041289
23	8	0.029248	–-2.229159	–0.945001
24	44	–0.00235	–0.222994	–0.546328
25	7	–2.141037	–0.197287	–0.722841
26	6	–4.92915	–0.213681	–1.099339
27	6	–2.719149	–1.03221	–1.611826
28	6	–2.943785	0.625716	–0.017813
29	6	–4.317661	0.641962	–0.177443
30	6	–4.086956	–1.064534	–1.821071
31	1	–2.0563	–1.69502	–2.151709
32	1	–2.468096	1.288482	0.689677
33	1	–4.905456	1.325091	0.422825
34	1	–4.489045	–1.760038	–2.546868
35	7	2.134213	–0.372024	–0.58217
36	6	4.92233	-0.6592	–0.80705

37	6	2.683539	–1.020514	–1.628489
38	6	2.961199	0.128394	0.354471
39	6	4.337619	0.005735	0.274494
40	6	4.051372	–1.175452	–1.770978
41	1	1.996459	–1.413726	–2.3631
42	1	2.508752	0.645424	1.187344
43	1	4.947202	0.434912	1.059866
44	1	4.430693	–1.700688	–2.638714
45	6	6.410258	–0.833459	–0.9158
46	1	6.942655	–0.032832	–0.400607
47	1	6.730225	–0.859664	–1.958616
48	1	6.709383	–1.780869	–0.455236
49	6	–6.415043	–0.20046	–1.315088
50	1	–6.68945	0.637736	–1.963865
51	1	–6.948113	–0.069888	–0.371458
52	1	–6.756748	–1.119233	–1.792445
53	8	1.187793	2.53108	–1.813962
54	8	0.198672	0.421459	–2.556324
55	1	0.640492	1.349623	–2.407232
56	1	–0.621834	0.550575	–3.049476

Table S6. Cartesian coordinates for $[Ru^{IV}(bda)(pic)_2(OH)]^+$ (Ru^{IV}-OH).

Center Number	Atomic Number	Coordinates (Å) x	y	z
1	44	–0.00313	–0.013848	–0.653645
2	7	–0.326927	1.236397	1.100793
3	6	–0.883649	2.849043	3.281499
4	6	–0.207313	0.739907	2.351615
5	6	–0.663611	2.520507	0.927654
6	6	–0.962163	3.358615	1.990335
7	6	–0.484831	1.530374	3.464769
8	1	–1.230679	4.385278	1.781662
9	1	–0.388682	1.118661	4.459336
10	1	–1.110852	3.471965	4.136721
11	7	0.343215	–1.186355	1.138164
12	6	0.935856	–2.717573	3.368932
13	6	0.685259	–2.475524	1.007717
14	6	0.237253	–0.645591	2.372552
15	6	0.531771	–1.395553	3.509285
16	6	1.002123	–3.272471	2.095933
17	1	0.444904	–0.949151	4.489672
18	1	1.273054	–4.304747	1.920563
19	1	1.176313	–3.308446	4.243047
20	6	–0.590661	2.959284	–0.50014
21	6	0.583646	–2.973841	–0.397951

22	8	0.130341	–2.054382	–1.201569
23	8	0.847003	–4.117667	–0.715854
24	8	–0.176499	2.002155	–1.278248
25	8	–0.851765	4.093567	–0.855567
26	7	2.122969	0.230909	–0.761645
27	6	4.899378	0.544335	–1.04147
28	6	2.804482	1.088269	0.020837
29	6	2.805907	–0.465878	–1.68955
30	6	4.17549	–0.335656	–1.850157
31	6	4.171869	1.268105	–0.091088
32	1	2.236713	1.646149	0.7514
33	1	4.669934	–0.92188	–2.614756
34	1	4.662004	1.976932	0.564579
35	7	–2.132815	–0.254153	–0.744457
36	6	–4.916362	–0.564195	–0.975311
37	6	–2.793068	–1.161465	0.00046
38	6	–2.844929	0.497717	–1.607523
39	6	–4.216939	0.369746	–1.744119
40	6	–4.162599	–1.337196	–0.085837
41	1	–2.205439	–1.757227	0.683424
42	1	–2.284379	1.21267	–2.193151
43	1	–4.732454	1.005903	–2.452631
44	1	–4.635333	–2.07936	0.545172
45	1	2.219103	–1.120972	–2.316271
46	6	6.38865	0.692136	–1.170081
47	1	6.729262	0.425675	–2.171373
48	1	6.891792	0.028042	–0.4595
49	1	6.70581	1.712094	–0.946534
50	6	–6.400386	–0.748994	–1.11317
51	1	–6.881035	0.1564	–1.485659
52	1	–6.854165	–1.026866	–0.160477
53	1	–6.610294	–1.554456	–1.824695
54	8	0.065095	–0.053462	–2.593915
55	1	–0.667396	–0.601216	–2.910064

Table S7. Cartesian coordinates for [(κ^3-bda)(pic)$_2$Ru^{IV}ORu^{IV}(κ^3-bda)(pic)$_2$] (Ru^{IV}–O–Ru^{IV}).

Center Number	Atomic Number	Coordinates (Å) x	y	z
1	44	-1.796897	-0.0706	-0.033232
2	7	-3.761545	-0.708002	-0.355394
3	6	-6.313811	-1.592935	-0.846182
4	6	-4.744817	-0.340878	0.489691
5	6	-4.002548	-1.486264	-1.422209
6	6	-5.27484	-1.953915	-1.709291
7	6	-6.051971	-0.78409	0.257445

8	1	-5.430195	-2.579113	-2.580437
9	1	-6.854129	-0.501258	0.927258
10	1	-7.324184	-1.940055	-1.031812
11	7	-2.947107	0.804899	1.583398
12	6	-4.610296	1.842133	3.562237
13	6	-2.432308	1.592336	2.544638
14	6	-4.291273	0.517134	1.584352
15	6	-5.136166	1.020376	2.561073
16	6	-3.257914	2.128422	3.549222
17	1	-6.191678	0.780431	2.544713
18	1	-2.808345	2.765438	4.302397
19	1	-5.258068	2.247298	4.332122
20	6	-2.771122	-1.772856	-2.228857
21	6	-0.93553	1.938201	2.597147
22	8	-0.237195	1.097818	3.20537
23	8	-0.638358	3.031022	2.070433
24	8	-1.689609	-1.198546	-1.721422
25	8	-2.768877	-2.455417	-3.23509
26	7	-2.276206	1.671828	-1.209621
27	6	-3.129092	3.9379	-2.649832
28	6	-2.686948	1.568002	-2.491502
29	6	-2.239879	2.901971	-0.651927
30	6	-2.658608	4.034433	-1.335773
31	6	-3.124275	2.65971	-3.223246
32	1	-2.651138	0.590346	-2.944069
33	1	-2.611314	4.993391	-0.82981
34	1	-3.454846	2.504638	-4.245136
35	7	-1.538523	-1.852039	1.178483
36	6	-1.380369	-4.144797	2.812398
37	6	-1.295448	-1.743347	2.503977
38	6	-1.668166	-3.092286	0.656359
39	6	-1.595392	-4.239241	1.430564
40	6	-1.216141	-2.855074	3.331453
41	1	-1.109326	-0.748244	2.894494
42	1	-1.812249	-3.166879	-0.410761
43	1	-1.70611	-5.203805	0.946158
44	1	-1.013757	-2.702518	4.386582
45	8	-0.000011	0.254518	-0.000014
46	1	-1.842026	2.987363	0.353841
47	44	1.796875	-0.070605	0.03324
48	7	3.76152	-0.707983	0.355454
49	6	6.313792	-1.592842	0.846345
50	6	4.744799	-0.340907	-0.489644
51	6	4.002517	-1.48617	1.422326
52	6	5.274813	-1.953778	1.709463
53	6	6.051956	-0.784084	-0.257345
54	1	5.430164	-2.578913	2.580654
55	1	6.854118	-0.501291	-0.92717
56	1	7.324167	-1.939934	1.032016
57	7	2.947101	0.804796	-1.583448

58	6	4.610304	1.84188	-3.562351
59	6	2.432313	1.592186	-2.544732
60	6	4.291265	0.517023	-1.584373
61	6	5.136164	1.020187	-2.561129
62	6	3.257928	2.128195	-3.549351
63	1	6.191674	0.780234	-2.544748
64	1	2.80837	2.765174	-4.302563
65	1	5.258082	2.246982	-4.332265
66	6	2.771076	-1.772751	2.228958
67	6	0.93555	1.938128	-2.597221
68	8	0.638474	3.031011	-2.070581
69	8	0.237139	1.097754	-3.205366
70	8	1.689553	-1.198531	1.721442
71	8	2.768826	-2.455244	3.235238
72	7	2.276187	1.671864	1.20958
73	6	3.129144	3.937949	2.649731
74	6	2.686813	1.568078	2.491501
75	6	2.240002	2.901981	0.651816
76	6	2.658767	4.034448	1.33563
77	6	3.124177	2.659793	3.223215
78	1	2.650868	0.590455	2.944126
79	1	2.611588	4.993381	0.829608
80	1	3.454652	2.504753	4.245141
81	7	1.538525	-1.852071	-1.178441
82	6	1.380398	-4.144834	-2.812348
83	6	1.668356	-3.092306	-0.656341
84	6	1.295289	-1.743392	-2.503907
85	6	1.215989	-2.855123	-3.331378
86	6	1.5956	-4.239266	-1.430542
87	1	1.812587	-3.166891	0.41076
88	1	1.013465	-2.702582	-4.386483
89	1	1.706473	-5.203821	-0.946155
90	1	1.842229	2.987348	-0.353984
91	6	-3.579682	5.146777	-3.422695
92	1	-4.383696	4.895443	-4.120789
93	1	-2.745363	5.54637	-4.013657
94	1	-3.923363	5.942267	-2.755753
95	6	-1.339166	-5.364301	3.690414
96	1	-0.945921	-6.230529	3.150604
97	1	-2.353156	-5.618005	4.025666
98	1	-0.729834	-5.192896	4.582113
99	6	3.579764	5.146837	3.422559
100	1	2.745347	5.546706	4.013195
101	1	3.923826	5.942155	2.755607
102	1	4.383505	4.89543	4.120939
103	6	1.339201	-5.364335	-3.690371
104	1	2.353159	-5.61787	-4.025847
105	1	0.729651	-5.193012	-4.581937
106	1	0.946209	-6.230633	-3.15049
107	1	1.109039	-0.748301	-2.894401

References

1. Bennett, M. A.; Smith, A. K. *J. Chem. Soc. Dalton Trans.* **1974**, 233.
2. Donnici, Claudio Luis; Máximo Filho, Daniel Henrique; Cruz Moreira, Leda Lúcia; Teixeira dos Reis, Genuína; Santos Cordeiro, Estefania; Ferreira de Oliveira, Ione Ma.; Carvalho, Sandra; Paniago, Eucler B. *J. Braz. Chem. Soc.* **1998**, *9*, 455.
3. Gray, A. P.; Kraus, H.; Heitmeier, D. E.; Shiley, R. H. *J Org Chem* **1968**, *33*, 3007.
4. Concepcion, J. J.; Binstead, R. A.; Alibabaei, L.; Meyer, T. J., *Inorg. Chem.* **2013**, *52*, 10744.
5. Gaussian 09, Revision D.01. M. J. Frisch, G. W. Trucks, H. B. Schlegel, G. E. Scuseria, M. A. Robb, J. R. Cheeseman, G. Scalmani, V. Barone, B. Mennucci, G. A. Petersson, H. Nakatsuji, M. Caricato, X. Li, H. P. Hratchian, A. F. Izmaylov, J. Bloino, G. Zheng, J. L. Sonnenberg, M. Hada, M. Ehara, K. Toyota, R. Fukuda, J. Hasegawa, M. Ishida, T. Nakajima, Y. Honda, O. Kitao, H. Nakai, T. Vreven, J. A. Montgomery, Jr., J. E. Peralta, F. Ogliaro, M. Bearpark, J. J. Heyd, E. Brothers, K. N. Kudin, V. N. Staroverov, T. Keith, R. Kobayashi, J. Normand, K. Raghavachari, A. Rendell, J. C. Burant, S. S. Iyengar, J. Tomasi, M. Cossi, N. Rega, J. M. Millam, M. Klene, J. E. Knox, J. B. Cross, V. Bakken, C. Adamo, J. Jaramillo, R. Gomperts, R. E. Stratmann, O. Yazyev, A. J. Austin, R. Cammi, C. Pomelli, J. W. Ochterski, R. L. Martin, K. Morokuma, V. G. Zakrzewski, G. A. Voth, P. Salvador, J. J. Dannenberg, S. Dapprich, A. D. Daniels, O. Farkas, J. B. Foresman, J. V. Ortiz, J. Cioslowski, and D. J. Fox, Gaussian, Inc., Wallingford CT, 2013.
6. Becke, A. D. *Phys. Rev., Ser. A* **1988**, *38*, 3098-3100.
7. Becke, A. D. *J. Chem. Phys.* **1993**, *98*, 1372-1377.
8. Becke, A. D. *J. Chem. Phys.* **1993**, *98*, 5648-5652.
9. Stevens, P. J.; Devlin, F. J.; Chablowski, C. F.; Frisch, M. J. *J. Phys. Chem.* **1994**, *98*, 11623-11627.
10. Lee, C.; Yang, W.; Parr, R. G. *Phys. Rev.* **1988**, *B37*, 785-789.
11. Hay, P. J.; Wadt, W. R. *J. Chem. Phys.* **1985**, *82*, 299.
12. Tomasi, J.; Mennucci, B.; Cammi, R. *Chem. Rev.* **2005**, *105* (8), 2999-3093.
13. Cance`s, E.; Mennucci, B.; Tomasi, J. *J. Chem. Phys.* **1997**, *107*, 3032.
14. Mennucci, B.; Cance`s, E.; Tomasi, J. *J. Phys. Chem. B* **1997**, *101*, 10506.
15. Cance`s, E.; Mennucci, B. *J. Math. Chem.* **1998**, *23*, 309.
16. Polyansky, D. E.; Muckerman, J. T.; Rochford, J.; Zong, R.; Thummel, R. P.; Fujita, E. *J. Am. Chem. Soc.* **2011**, *133*, 14649.
17. Kelly, C. P.; Cramer, C. J.; Truhlar, D. G. *J. Phys. Chem. B* **2006**, *110*, 16066-16081.
18. Kelly, C. P.; Cramer, C. J.; Truhlar, D. G. *J. Phys. Chem. B* **2007**, *111*, 408-422.
19. Stratmann, R. E.; Scuseria, G. E.; Frisch, M. J. *J. Chem. Phys.* **1998**, *109*, 8218-8224.
20. Bauernschmitt, R.; Ahlrichs, R. *Chem. Phys. Lett.* **1996**, *256*, 454-464.
21. Casida, M. E.; Jamorski, C.; Casida, K. C.; Salahub, D. R. *J. Chem. Phys.* **1998**, *108*, 4439-4449.
22. Sheldrick, G. M.; Siemens Analytical Instruments, Inc.: Madison WI, 1994.

23. Sheldrick; Bruker AXS Inc.: 2007.